

# Flux Dynamics and Thermal Behavior of a GdBaCuO Bulk Magnetized by Single- and Double-Pulse Techniques using a Split-Type Coil

Tatsuya Hirano, Hiroyuki Fujishiro, Tomoyuki Naito, Mark D. Ainslie, *Senior Member, IEEE*, and Yun-Hua Shi

**Abstract**—We have investigated the trapped field properties of a GdBaCuO disk bulk during single- and double- pulsed field magnetization (PFM) using a split-type coil for various pulse sequences for the first time. It is well known that the multi-PFM technique using a solenoid-type coil and the single-PFM technique using a split-type coil are effective to enhance the trapped field due to a lower temperature rise. However, it was found, in this work, that the trapped field by double-PFM using the split-type coil was not enhanced in spite of lower temperature rise. We analyzed the magnetizing process using two parameters, the “magnetic flux penetration ratio”,  $R_{in}$ , and the “magnetic flux residual ratio”,  $R_{out}$ , for various pulse sequences for the split-type and solenoid-type coils. The  $R_{in}$  value was decreased by the double-PFM for both coils, and the  $R_{out}$  value was improved only by the double-PFM using the solenoid-type coil. As a result, the trapped field for single-PFM using the split-type coil, which has a higher  $R_{in}$ , reduced after the double-PFM due to a decrease of  $R_{in}$  and no enhancement of  $R_{out}$ . These results are in clear contrast to those using the solenoid-type coil.

**Index Terms**—Bulk high-temperature superconductors, multi-pulse application, pulsed field magnetization, REBaCuO bulk, split-type coil, trapped field magnets

## I. INTRODUCTION

REBaCuO (RE: rare earth element or Y) superconducting bulks have been used as a trapped field magnet (TFM) that can provide a magnetic field of several Tesla for engineering applications such as rotating machines [1], magnetic separation [2], and a magnetic drug delivery system [3]. The pulsed field magnetization (PFM) technique is a magnetizing method for superconducting bulks with a compact, mobile and inexpensive setup, compared to field-cooled magnetization (FCM). However, the trapped field by PFM is generally much lower than that by FCM because of a large temperature rise associated with the rapid and dynamical motion of magnetic flux [4]. The PFM technique consists of an ascending (flux

penetration) phase on the order of milliseconds and then a descending (flux flow) phase. To enhance the trapped field by PFM, a large amount of flux penetration and a small amount of flux flow should be achieved. There have been several approaches to enhance the trapped field by PFM using the solenoid-type coil. Multi-pulsed field magnetization techniques, which involve iteratively applying pulsed fields, are effective, such as the successive pulse application (SPA) [5] and the multi-pulse technique with step-wise cooling (MPSC) [6]. The multi-PFM technique achieves a reduction in flux flow from lowering the flux pinning and viscous losses due to the already trapped magnetic flux after the 1<sup>st</sup> magnetic pulse [7]. Using a modified MPSC (MMPSC) technique, a record-high trapped field of 5.20 T was achieved using a solenoid-type coil with a 45 mm GdBaCuO disk bulk at 30 K [8]. Similarly, there have been reports to enhance the trapped field by PFM using a split-type coil with an iron yoke [9], in which the flux intrudes by a flux jump with reduced flux flow. The cooling of the bulk for the split-type coil is faster than that for the solenoid-type coil because the bulk is cooled from the periphery along the *ab*-plane, which has higher thermal conductivity than the *c*-axis [9]. However, multi-pulse effects using the split-type coil have not yet been reported.

In this study, we investigated the trapped field properties of a GdBaCuO disk bulk during single- and double-PFM using the split-type coil for various sequences. To understand the double-pulse effect, we compared the trapped field properties to those using the solenoid-type coil.

## II. EXPERIMENTAL SETUP

A GdBaCuO superconducting disk bulk of 41 mm in diameter and 12 mm in thickness was grown using the top-seeded melt-growth (TSMG) process at the University of Cambridge [10]. Fig. 1 shows the schematic view of the experimental setup for the PFM. The split-type coil (72 mm in inner diameter (I.D.), 124 mm in outer diameter (O.D.), and 35 mm in height (H)) and the solenoid-type coil (99 mm I.D., 121 mm O.D. and 50 mm H) are used as magnetizing coils. The bulk was fastened in a brass sample holder using a thin indium sheet and was cooled from the periphery along the *ab*-plane. A pair of permendur yokes (60 mm diameter and 65 mm H) was inserted in the bores of the split-type coil [9]. For the solenoid-type coil, the same bulk was mounted in a stainless steel ring 17.5 mm in width and cooled from the bottom surface along

This research is partially supported from JSPS KAKENHI Grant No. 15K04646. M. D. Ainslie would like to acknowledge financial support from an Engineering and Physical Sciences Research Council (EPSRC) Early Career Fellowship EP/P020313/1. All data are provided in full in the results section of this paper.

T. Hirano, H. Fujishiro and T. Naito are with the Department of Physical Science and Materials Engineering, Faculty of Science and Engineering, Iwate University, Morioka 020-8551, Japan (e-mail: g0318132@iwate-u.ac.jp, fujishiro@iwate-u.ac.jp).

M. D. Ainslie and Yun-Hua Shi are with Bulk Superconductivity Group, Department of Engineering, University of Cambridge, Cambridge CB2 1PZ, UK (e-mail: mark.ainslie@eng.cam.ac.uk).

the  $c$ -axis of the bulk, where a soft iron yoke (60 mm in diameter and 20 mm in H) is installed underneath the bulk [4].

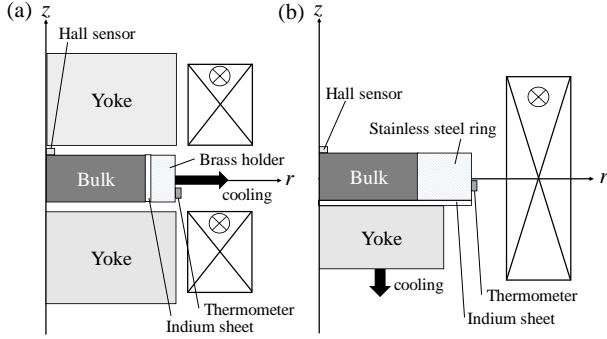


Fig. 1. Schematic view of the experimental setup for the PFM experiments using (a) the split-type coil and (b) the solenoid-type coil.

Fig. 2 shows the time sequences of the operating temperature settings used in this study. For the single-pulse application, shown in Figs. 2(a) and 2(b), the bulk was cooled to  $T_{s1} = 65$  or 25 K, and a single-magnetic pulse with a rise time of 18 ms (split-type coil) or 13 ms (solenoid-type coil),  $B_{ex1}$ , ranging from 3 to 6 T was applied to the bulk. For the double-pulse application, shown Figs. 2(c) and 2(d), the 1<sup>st</sup> pulse of  $B_{ex1} = 3$  T was applied at  $T_{s1} = 65$  K for all cases. In the 2<sup>nd</sup> stage, the bulk was cooled to  $T_{s2} = 65$  or 25 K and the 2<sup>nd</sup> pulse,  $B_{ex2}$ , ranging from 3 to 6 T was applied to the bulk. The magnetic pulse and temperature sequences for each magnetizing coil are named as follows.

1. Single pulse using split-type coil: S-sp( $T_{s1}$ )
2. Double pulse using split-type coil: D-sp( $T_{s1}, T_{s2}$ )
3. Single pulse using solenoid-type coil: S-sol( $T_{s1}$ )
4. Double pulse using solenoid-type coil: D-sol( $T_{s1}, T_{s2}$ )

During the PFM process, the time evolution of the magnetic field,  $B(t)$ , at the center of the bulk surface was measured using a Hall sensor (F. W. Bell, BHT921).  $B(t)$  at 300 ms is defined as the trapped field,  $B_t$ . The time evolution of the temperature,  $T(t)$ , was measured by a CERNOX<sup>TM</sup> thermometer on the side surface of the brass holder for the split-type coil

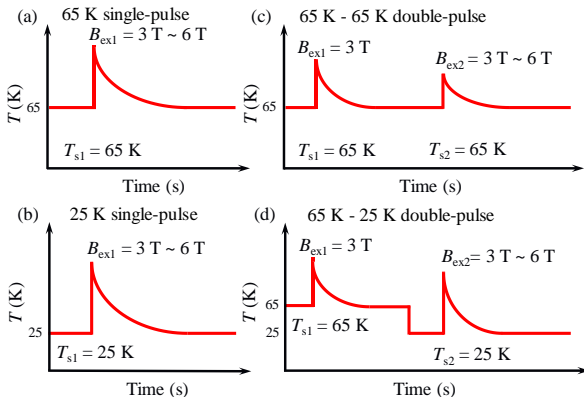


Fig. 2. Time sequences of the operating temperature settings used in this study for (a) 65 K single pulse, (b) 25 K single pulse, (c) 65 K - 65 K double pulse and (d) 65 K - 25 K double pulse.

and on the side surface of stainless steel ring for the solenoid-type coil.

### III. RESULTS

Fig. 3(a) shows the applied pulsed field ( $B_{ex}$ ) dependence of the trapped field,  $B_t$ , at the center of the bulk surface using the split-type coil for various sequences. Here, the applied field, at which the  $B_t$  value begins to increase, is defined as the rise field,  $B_r$ . The  $B_t$  value for S-sp(65 K) increases from  $B_r = 3.06$  T by the flux jump and the highest  $B_t$  value of 2.79 T was achieved at  $B_{ex} = 3.76$  T. The  $B_t$  value for S-sp(25 K) increased from  $B_r = 4.17$  T and a highest  $B_t$  of 3.96 T was achieved at  $B_{ex1} = 5.43$  T. These rapid increases in  $B_t$  above  $B_r$  result from flux jumps [11], [12] (or so-called giant flux leaps (GFLs) in other works [13]), which are a characteristic behavior when using the split-type coil. The rise field,  $B_r$ , increased and the trapped field,  $B_t$ , was usually enhanced when lowering the operating temperature during single-PFM [14]. These results were also obtained for the 2<sup>nd</sup> pulse application of the D-sp(65 K, 65 K) and D-sp(65 K, 25 K). It should be noted that the rise field,  $B_r$ , of the 2<sup>nd</sup> pulse application increased, but the maximum  $B_t$  value was not enhanced, compared to that of single-pulse application.

On the other hand, for the solenoid-type coil, as shown in Fig. 3(b), the  $B_t$  value for S-sol(65 K) increases monotonically with increasing  $B_{ex}$ . When  $B_{ex}$  is 4.0 T, the  $B_t$  value for D-sol(65 K, 65 K) is higher than that for S-sol(65 K), which indicates that the flux jump also occurs for the double-PFM. These results are similar to that for S-sol(25 K) and D-sol(65 K, 25 K). These results support the previous reports, in which the multi-PFM using the solenoid-type coil enhances the trapped field [8], [15].

Fig. 4(a) shows the maximum temperature rise,  $\Delta T_{max}$ , during PFM, as a function of the applied pulsed field ( $B_{ex}$ ), for each sequence using the split-type coil.  $\Delta T_{max}$  increased with increasing  $B_{ex}$  for all cases. The  $\Delta T_{max}$  value of the double-PFM is lower than that of the single-PFM, which results from lowering the flux pinning and viscous losses due to the already trapped magnetic flux after the 1<sup>st</sup> magnetic pulse application [7], [15]. The  $\Delta T_{max}$  value using the solenoid-type coil, shown in Fig. 4(b), is larger than that using the split-type coil, because the bulk is cooled via the  $c$ -axis (solenoid-type coil) of lower thermal conductivity, rather than the  $ab$ -plane (split-type coil) [9].

Figs. 5(a) and 5(b) show the time evolutions of the applied field,  $B_{ex}(t)$ , and trapped field,  $B(t)$ , at the center of the bulk surface for S-sp(25 K) for  $B_{ex1} = 4.17$  T and S-sol(25 K) for  $B_{ex1} = 4.14$  T, respectively. In Fig. 5(a), the magnetic flux doesn't intrude into the center of the bulk for the split-type coil. In Fig. 5(b), for the solenoid-type coil,  $B(t)$  takes a peak value of  $B_{in} = 2.13$  T, which is defined as the maximum penetration field, and then decreases to a final small  $B_t$  value due to a large flux flow.

Figs. 5(c) and 5(d) show similar plots for S-sp(25 K) for  $B_{ex1} = 4.89$  T and D-sp(65 K, 25 K) for  $B_{ex2} = 4.99$  T, respectively. In Fig. 5(c), with increasing  $B_{ex1}$ , compared to Fig. 5(a), the magnetic flux intruded rapidly via a flux jump and the  $B(t)$  reached  $B_{in} = 4.67$  T. After that,  $B(t)$  gradually decreased to  $B_t = 3.40$  T, where the flux flow, defined as  $\Delta B (= B_{in} - B_t)$ , was

1.27 T. For D-sp(65 K, 25 K), shown in Fig. 5(d), after the 1<sup>st</sup> pulse of  $B_{ex1} = 3$  T was applied at 65 K, the magnetic flux also intruded the bulk center suddenly via a flux jump and then flow out of the bulk to the final value,  $B_t$ . The  $B_{in}$  and  $B_t$  values were slightly smaller than those for S-sp(25 K) as shown in Fig. 5(c) at a nearly identical applied field. The final  $B_t$  reduction mainly results from the decrease in  $B_{in}$  for the double-PFM.

Figs. 5(e) and 5(f) show similar plots for S-sol(25 K) for  $B_{ex1} = 5.56$  T and D-sol(65 K, 25 K) for  $B_{ex2} = 5.57$  T. When  $B_{ex1}$  is increased, as shown in Fig. 5(e), the  $B_{in}$  and  $B_t$  values increase, compared to those in Fig. 5(b). For D-sol(65 K, 25 K) in Fig. 5(f), after the 1<sup>st</sup> pulse of  $B_{ex1} = 3$  T was applied at 65 K, the  $B_{in}$  value was smaller than that for S-sol(25 K). This result is consistent with that obtained using the split-type coil. The  $B_t$  value for D-sol(65 K, 25 K) was also higher than that for S-sol(25 K). This is in contrast with the double-pulse effect using the split-type coil. The enhancement of the final  $B_t$  mainly results from the decrease in the flux flow ( $\Delta B$ ) for the double-PFM.

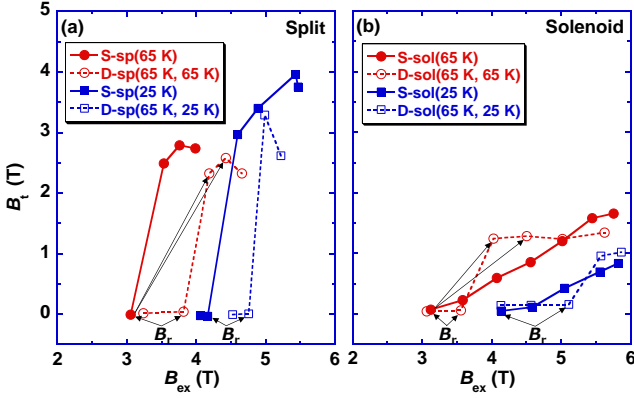


Fig. 3. Applied pulsed field ( $B_{ex}$ ) dependence of the trapped field,  $B_t$ , at the center of the bulk surface using (a) the split-type coil and (b) the solenoid-type coil for various sequences. The applied field, at which the  $B_t$  value begins to increase, is defined as the rise field,  $B_r$ .

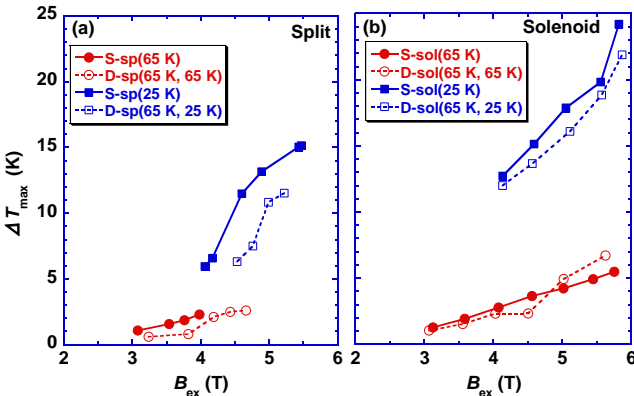


Fig. 4. Maximum temperature rise,  $\Delta T_{max}$ , during PFM, as a function of applied pulsed field ( $B_{ex}$ ), for each sequence using (a) the split-type coil and (b) the solenoid-type coil.

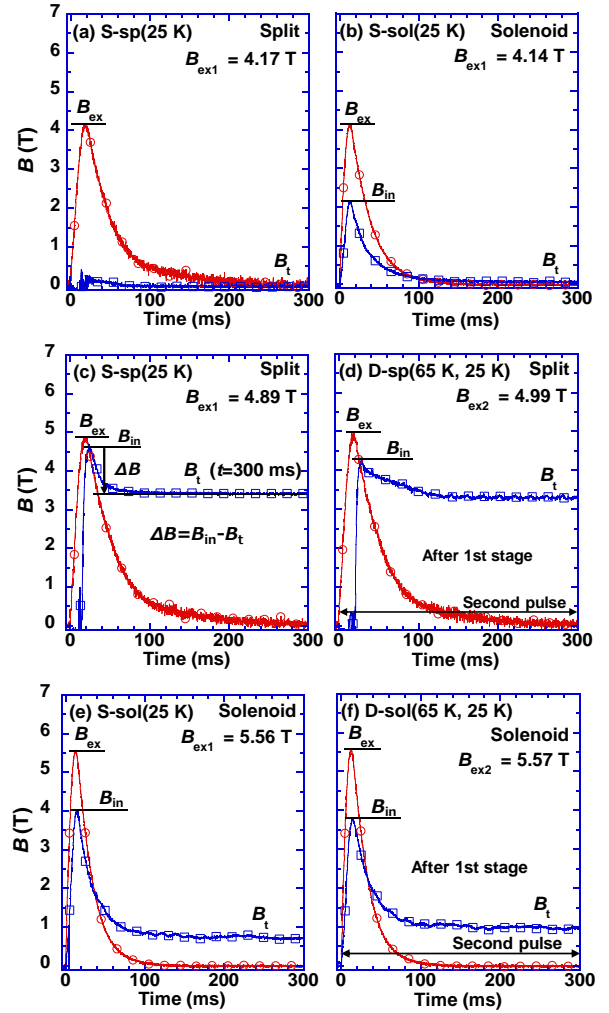


Fig. 5. Time evolution of the applied field,  $B_{ex}(t)$ , and trapped field,  $B_t(t)$  at the center of the bulk surface for (a) S-sp(25 K) for  $B_{ex1} = 4.17$  T, (b) S-sol(25 K) for  $B_{ex1} = 4.14$  T, (c) S-sp(25 K) for  $B_{ex1} = 4.89$  T, (d) D-sp(65 K, 25 K) for  $B_{ex2} = 4.99$  T, (e) S-sol(25 K) for  $B_{ex1} = 5.56$  T and (f) D-sol(65 K, 25 K) for  $B_{ex2} = 5.57$  T.

#### IV. DISCUSSION

Using the experimental results, we now discuss the double-pulse effect during PFM using the split-type coil, compared with single-PFM and the solenoid-type coil. Fig. 6 shows the applied field ( $B_{ex}$ ) dependence of the “magnetic flux penetration ratio”,  $R_{in}$ , using the split-type and solenoid-type coils during single- and double-PFM. Here,  $R_{in}$  is defined as  $B_{in}/B_{ex}$ .  $R_{in} = 1.0$  corresponds to an ideal flux penetration during FCM using the Bean model [16]. The  $R_{in}$  value of S-sp increases rapidly and takes a maximum of higher than 0.9 ~ 0.95 by the assistance of a flux jump, shown in Fig. 4(a). The  $R_{in}$  value for D-sp is nearly equal to or slightly smaller than that for S-sp because of the existence of a trapped flux after the 1<sup>st</sup> pulse. Using the solenoid-type coil,  $R_{in}$  gradually increases with increasing  $B_{ex}$  due to the absence of flux jumps and is smaller than that for the split-type coil. Similarly to the split-type coil,  $R_{in}$  for D-sol is smaller than that for S-sol. The double-PFM by both magnetizing coils results in a decreased  $R_{in}$  value, because it is more difficult for

the flux to penetrate the bulk due to the existence of the flux trapped from the 1<sup>st</sup> pulse [15].

Fig. 7(a) shows the “magnetic flux residual ratio”,  $R_{out}$ , using the split-type and solenoid-type coils during single- and double-PFM, as a function of  $B_{in}$ . Here,  $R_{out}$  is defined as  $B_t/B_{in}$ , which is the ratio of the trapped field,  $B_t$ , to the maximum penetration field,  $B_{in}$ . The  $R_{out}$  value increases concomitantly with increasing  $B_{ex}$  using the split-type coil, and becomes a maximum. And then the  $R_{out}$  value decreases with a further increase in  $B_{ex}$ , which indicates that the flux flow,  $\Delta B$ , becomes large due to the large temperature rise [17]. The maximum value of  $R_{out}$  is not enhanced by double-PFM using split-type coil. The  $B_{in}$  for D-sp(65 K, 25 K) is smaller than that for S-sp(25 K) when the maximum  $R_{out}$  is achieved. The temperature rise of  $\Delta T_{max} = 10.8$  K (D-sp(65 K, 25 K)) and  $\Delta T_{max} = 15.0$  K (S-sp(25 K)) was measured at the maximum  $R_{out}$  for each PFM, as shown in Fig. 4(a). These results suggest that  $R_{out}$  does not strongly depend on temperature rise. The reduction of the trapped field after the 2<sup>nd</sup> pulse using the split-type coil can be mainly explained by the reduction of both  $R_{in}$  and  $R_{out}$ . On the other hand, for the solenoid-type coil, the  $R_{out}$  value for D-sol(65 K, 25 K) is larger than that for S-sol(25 K) at  $B_{in}$  higher than 3.11 T, which is a different result when using the split-type coil, although the  $R_{in}$  value is small. The trapped field enhancement after the 2<sup>nd</sup> pulse using the solenoid-type coil, as shown in Fig. 3, can be mainly explained by the enhancement of  $R_{out}$ .

Fig. 7(b) shows applied field ( $B_{ex}$ ) dependence of  $R_{in} \times R_{out}$  using the split-type and solenoid-type coils during single- and double-PFM. The  $R_{in} \times R_{out}$  value is equivalent to the magnetic flux trapping ratio ( $B_t/B_{ex}$ ), which was rewritten from Figs. 3(a) and 3(b). The higher  $R_{in} \times R_{out}$  value approaches an ideal PFM process. The  $R_{in} \times R_{out}$  values for D-sp(65 K, 25 K) are smaller than those for S-sp(25 K) in spite of a low temperature rise, because of the decrease of  $R_{in}$  and/or  $R_{out}$ . On the other hand, for the solenoid-type coil, the  $R_{in} \times R_{out}$  value for D-sol(65 K, 25 K) increases for higher  $B_{ex}$ , compared to that for S-sol(25 K) because of the enhanced  $R_{out}$  value.

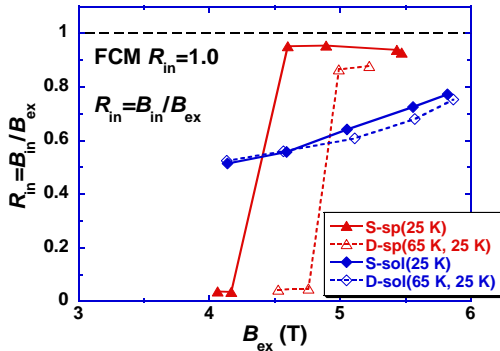


Fig. 6. Applied field ( $B_{ex}$ ) dependence of the magnetic flux penetration ratio,  $R_{in}$ , using the split-type and solenoid-type coils at 25 and 65 K to 25 K during single- and double-PFM.

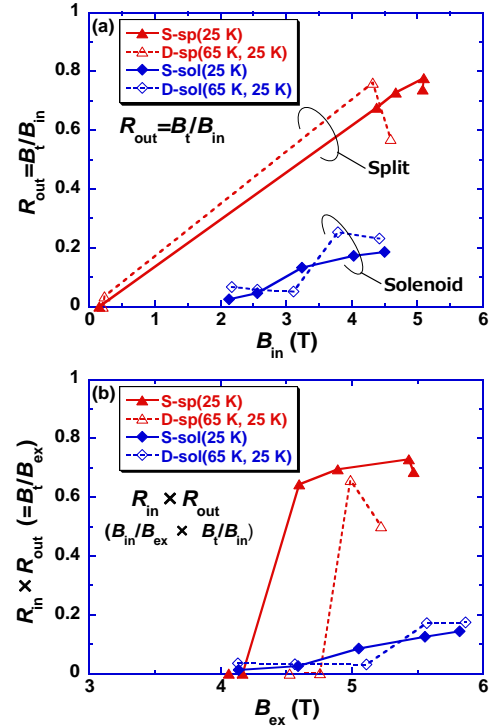


Fig. 7. (a) Magnetic flux residual ratio,  $R_{out}$ , for each sequence, as a function of  $B_{in}$ . (b)  $R_{in} \times R_{out}$  value ( $= B_t/B_{ex}$ ) for each sequence, as a function of  $B_{ex}$ .

## V. CONCLUSION

We have experimentally investigated the trapped field properties of a GdBaCuO disk bulk during single and double pulsed-field magnetization (PFM) using a split-type coil for various sequences for the first time. The important results and conclusion obtained in this study are summarized as follows.

1. The trapped field by double-PFM using the split-type coil was not enhanced in this study, although a lower temperature rise was achieved. These results are in clear contrast with those of the multi-PFM technique using a solenoid-type coil.
2. The magnetizing process was analyzed using the parameters of “magnetic flux penetration ratio”,  $R_{in}$ , and “magnetic flux residual ratio”,  $R_{out}$ , for various sequences using the split-type and solenoid-type coils. The double-PFM by both coils resulted in a decreased  $R_{in}$  value because of the already trapped flux after the 1<sup>st</sup> pulse. For the solenoid-type coil, the  $R_{out}$  value was enhanced by the double-PFM due to the lower temperature rise. The trapped field during single-PFM using the split-type coil, which exhibits a high  $R_{in}$ , was decreased by the double-pulse application due to the decrease of  $R_{in}$  and no enhancement of  $R_{out}$ .

## REFERENCES

- [1] D. Zhou *et al.*, “An overview of rotating machine systems with high-temperature bulk superconductors,” *Supercond. Sci. Technol.*, vol. 25, no. 12, Oct. 2012, Art. no. 103001.
- [2] K. Yokoyama *et al.*, “Solid-liquid magnetic separation using bulk superconducting magnets,” *IEEE Trans. Appl. Supercond.*, vol. 13, no. 2, pp.1592-1595, Jul. 2003.

- [3] S. Nishijima *et al.*, “Research and Development of Magnetic Drug Delivery System Using Bulk High Temperature Superconducting Magnet,” *IEEE Trans. Appl. Supercond.*, vol. 19, no. 3, pp.2257-2260, Jun. 2009.
- [4] M. D. Ainslie *et al.*, “Modelling and comparison of trapped fields in (RE)BCO bulk superconductors for activation using pulsed field magnetization,” *Supercond. Sci. Technol.*, vol. 27, no. 6. Jun. 2014, Art. no. 065008.
- [5] H. Fujishiro, T. Tateiwa, K. Kakehata, T. Hiyama and T. Naito, “Trapped field and temperature rise on a  $\Phi$  65 mm GdBaCuO bulk by pulsed field magnetization,” *Supercond. Sci. Technol.*, vol. 20, no. 10, pp. 1009-1014, Oct. 2007.
- [6] M. Sander, U. Sutter, R. Koch and M. Klaser, “Pulsed magnetization of HTS bulk parts at  $T < 77$  K,” *Supercond. Sci. Technol.*, vol. 13, no. 6, pp. 841-845, Jun. 2000.
- [7] H. Fujishiro *et al.*, “Pulsed field magnetization of GdBaCuO bulk with stronger pinning characteristics,” *IEEE Trans. Appl. Supercond.*, vol. 19, no. 3, pp. 3545–3548, Jun. 2009.
- [8] H. Fujishiro, T. Tateiwa, A. Fujiwara, T. Oka and H. Hayashi, “Higher trapped field 5 T on HTSC bulk by modified pulse field magnetizing,” *Physica C*, vol. 445-448, pp. 334-338, Oct. 2006.
- [9] M. D. Ainslie *et al.*, “Enhanced trapped field performance of bulk high-temperature superconductors using split coil, pulsed field magnetization with an iron yoke,” *Supercond. Sci. Technol.*, vol. 29, no. 7, Jul. 2016, Art. no. 074003.
- [10] Y. Shi, N. H. Babu, D. A. Cardwell, “Development of a generic seed crystal for the fabrication of large grain (RE)-Ba-Cu-O bulk superconductors,” *Supercond. Sci. Technol.*, vol. 18, no. 4, pp. L13-L16, Apr. 2005.
- [11] R. Weinstein, D. Parks, R-P. Sawh, K. Carpenter, K. Davey, “Anomalous results observed in magnetization of bulk high temperature superconductors-A windfall for applications,” *J. Appl. Phys.* 119, 2016, Art. no. 133906.
- [12] D. Zhou *et al.*, “Exploiting flux jumps for pulsed field magnetization,” *Supercond. Sci. Technol.*, vol. 31, no. 10, Oct. 2018, Art. no. 105005.
- [13] R. Weinstein, D. Parks, R-P. Sawh, K. Davey, K. Carpenter, “Observation of a Bean model limit a large decrease in required applied activation field for TFM,” *IEEE Trans. Appl. Supercond.*, vol. 25, no. 3, Jun. 2015, Art. no. 6601106.
- [14] K. Yokoyama, M. Kaneyama, H. Fujishiro, T. Oka and K. Noto, “Temperature rise and trapped field in a GdBaCuO bulk superconductor cooled down to 10 K after applied pulsed magnetic field,” *Physica C*, vol. 426-431, pp. 671-675, Oct. 2005.
- [15] M. D. Ainslie *et al.*, “Toward optimization of multi-pulse, pulsed field magnetization of bulk high temperature superconductors,” *IEEE Trans. Appl. Supercond.*, vol. 28, no. 4, Jan. 2018, Art. no. 6800207.
- [16] C. P. Bean, “Magnetization of hard superconductors,” *Phys. Rev. Lett.*, vol. 8, pp. 250-253, Mar. 1962.
- [17] H. Ikuta, *et al.*, “Pulsed field magnetization of melt-processed Sm-Ba-Cu-O”, *Supercond. Sci. Technol.*, vol. 13, no. 6, pp. 846-849, Jun. 2000.